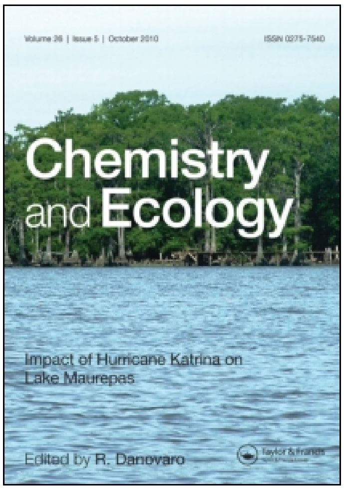

Chemistry and Ecology
Publication details, including instructions for authors and subscription information:
http://www.informaworld.com/smpp/title~content=t713455114

Combined molecular mechanics, molecular dynamics and quantum mechanical study of (+)-multifidene structure and conformation

Tiziana Marino[a]; Nino Russo[a]; Emilia Sicilia[a]
[a] Dipartimento di Chimica e Centro di Calcolo ad Alte Prestazioni per Elaborazioni Parallele e Distribuite-Centro d'Eccellenza MIUR, Università della Calabria, Arcavacata di Rende (CS), Italy

To cite this Article Marino, Tiziana , Russo, Nino and Sicilia, Emilia(2004) 'Combined molecular mechanics, molecular dynamics and quantum mechanical study of (+)-multifidene structure and conformation', Chemistry and Ecology, 20: 3, 157 — 165

To link to this Article: DOI: 10.1080/02757540410001690324

URL: http://dx.doi.org/10.1080/02757540410001690324

Chemistry and Ecology
June 2004, Vol. 20(3), pp. 157–165

COMBINED MOLECULAR MECHANICS, MOLECULAR DYNAMICS AND QUANTUM MECHANICAL STUDY OF (+)-MULTIFIDENE STRUCTURE AND CONFORMATION

TIZIANA MARINO, NINO RUSSO* and EMILIA SICILIA

Dipartimento di Chimica e Centro di Calcolo ad Alte Prestazioni per Elaborazioni
Parallele e Distribuite-Centro d'Eccellenza MIUR, Università della Calabria,
I-87030 Arcavacata di Rende (CS), Italy

(In final form 18 February 2004)

Molecular mechanics, molecular dynamics and quantum mechanical tools have been used to explore the conformational space of (+)(3S,4S)-multifidene bioactive compounds. All the computations have been performed in the absence and presence of the solvent, simulated by the explicit introduction of a number of water molecules or by the polarized continuum model (PCM). Three conformational minima, both *in vacuo* and in water (simulated by PCM tool), have been confirmed at *ab initio* level of theory (B3LYP and MP2). All minima lie in a very narrow range of energy, and the interconversion between them is possible with a small amount of energy expense.

Keywords: Multifidene; Density functional theory; Second-order Moller-Plesset; Molecular dynamics; Solvent effects

1 INTRODUCTION

In the evolution history of living organisms, one of the first communication modes between individuals has certainly been that in which chemical signals have been employed. These chemical signals, which allow information transfer between members of the same species, are known as pheromones. Both plants and animals use this tool, especially to induce the sexual cycle. Chemists have studied the pheromones of insects with different aims and scopes related to important industrial uses. Less attention has been dedicated to the pheromones produced by the vegetal kingdom, and very few studies have examined marine organisms (Boland, 1995; Bradley, 1999). (+)-3S,4S-Multifidene (multifidene) is a molecule that *Cutleria multifidia* and *Chorda tomentosa* brown algae discharge into sea water to attract swimming males (Boland *et al.*, 1981). A number of studies have been dedicated to the synthesis of this bioactive molecule to produce analogues with the highest biological activity and lower synthetic costs (Crouse and Paquette, 1981; Burks and Crandall, 1984; Boland

---

* Corresponding author. E-mail: nrusso@unical.it

ISSN 0275-7540 print; ISSN 1029-0370 online
DOI: 10.1080/02757540410001690324

et al., 1995; Hemamalini and Scheffold, 1995; Randall *et al.*, 1995; Lebreton *et al.*, 1996; Randall and Snapper, 1998; Stanley and Wan, 1998; Bradley, 1999; Ellis and King, 2002). The main motivation for these investigations is to obtain a certain quantity of pheromones for use in anti-pollution activities, *e.g.*, cleaning beaches that have abnormal amounts of algae as a result of increased pollution in the marine environment. Furthermore, they can be used to produce large amounts of algae in controlled coastal sites for use as biomass for energy production. In spite of these experimental studies, a rational strategy to obtain powerful synthetic analogues requires accurate knowledge of the structural features, conformational behaviour and electronic characteristics of multifidene. This information is also essential for studying the action mechanism and in designing the active site of the receptor (Boland *et al.*, 1983b). Apart from a previous study on the conformation of multifidene, performed at an empirical level (Albano *et al.*, 1991), no such information is available in the literature.

In this work, we have studied in detail the structural and conformational behaviour of multifidene by using a variety of theoretical tools, ranging from classical molecular mechanics and dynamics to modern quantum-mechanical approaches such as the density functional (DFT) theory and Moller-Plesset second-order perturbation (MP2) theory. The investigation was performed *in vacuo* and redone in water in order to take into account the solvent effects on the examined molecular properties.

2 COMPUTATIONAL DETAILS

Molecular mechanics (MM) and molecular dynamics (MD) computations were carried out using the consistent valence force field (CVFF) (Dauber-Osguthorpe *et al.*, 1988) as implemented in the Insight/Discover codes (Biosym Technologies, San Diego, CA), while DFT and MP2 computations were carried out using the Gaussian-98 package (Frisch *et al.*, 1998). The solvent was simulated by placing the multifidene in an equilibrated three-dimensional grid solvent in a simulation box of 22 Å side with 288 water molecules for both MM and MD calculations. MD simulations were obtained at constant temperature (300 K) and volume (NVT ensemble), and the temperature was controlled throughout direct bath-temperature coupling to obtain a broader sampling of the conformational space. The MD simulation time consisted of 2.5 ns with a time steep of 1 fs. This interval was long enough to span the equilibration state regions. The quenching procedure (Villa *et al.*, 1995; Marino *et al.*, 2001) was applied after 500 ps of simulation, and snapshots were taken every about 30 ps. A total of 60 frames were selected from both water and *in vacuo* dynamics. All these structures were optimized with the conjugate-gradient algorithm with convergence criteria of 0.001 kcal Å^{-1}.

Both DFT and MP2 quantum mechanical calculations were performed by using the 6-311++G** orbital basis sets, fully optimizing the geometries of the minima and transition states. In DFT computations, the hybrid Becke3 (B3; Becke, 1993) and Lee Yang and Parr (LYP; Lee *et al.*, 1988) exchange-correlation functional were used. In all cases, the solvent effects were introduced by the Polarizable Continuum Model (PCM; Tomasi and Persico, 1994; Barone *et al.*, 1998; Barone and Cossi, 1998). All the energetic parameters included the zero-point energy corrections obtained from the harmonic vibrational frequencies.

3 RESULTS AND DISCUSSION

The chain of multifidene is characterized by the presence of three dihedral angles (τ_1, τ_2 and τ_3 as depicted in Fig. 1) other than a five-member ring with a double bond between C5 and C1

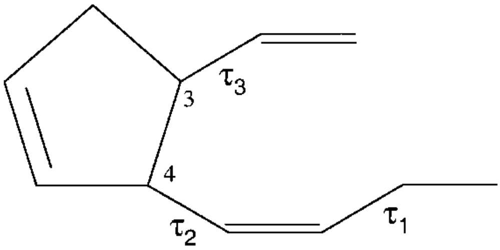

FIGURE 1 Multifidene chain showing the three dihedral angles.

atoms and two centres of well-defined chirality (S) on the C3 and C4 atoms of the ring (Fig. 1; Boland *et al.*, 1983a; Paquette *et al.*, 1984). As a first step, the conformational space was explored using the MM methods. A series of energy maps as a function of τ_1 and τ_2 (varied in steps of 10 degrees each) were obtained, fixing the τ_3 angle at values ranging from −180 to 180° with a step of 10°. The computations showed the existence of six conformational minima in an energetic range of only few kcal per mol. All these minima were fully minimized, and the results are listed in Table I. The absolute minimum is characterized by τ_1, τ_2 and τ_3 values of 170, 120 and −60°, respectively. The geometry of the absolute minimum was selected as the starting point of MD simulations *in vacuo* and in the solvent. The energy and τ_1, τ_2 and τ_3 variations during the simulation time are shown in Figures 2 and 3 *in vacuo* and in the solvent, respectively. In both MD simulations, the energy variation was smaller, while the dihedral angles showed many fluctuations. In particular, τ_1 varied from −180 to 180°, while τ_2 and τ_3 remained around 60 and −80°, respectively.

The 60 frames obtained from the quenching procedure of the MD trajectory *in vacuo* and in the solvent were fully minimized, with five conformers *in vacuo* and six in water. The relative energies and dihedral angle values are listed in Table II. As shown in the table, the energy differences between the absolute and relative minima (ΔE) were very small *in vacuo* (maximum 2.1 kcal mol^{-1}) and became more pronounced in the presence of water. Furthermore, we note a pronounced difference between the absolute minimum *in vacuo* with respect to the corresponding solvated minimum. In particular, in the former, the lateral chains assumed a more closed shape, while in the latter a more transoid form resulted. In both cases, the five-membered ring was almost planar.

A comparison between the MM minima *in vacuo* obtained before and after the MD simulations reveals some differences in the stability order of the conformers but both agree in the prediction of the absolute minimum.

As a second step, we have computed at the quantum-mechanical level (using both the B3LYP and MP2 tools) the most stable conformations coming from the MM and MD

TABLE I Relative energies (ΔE in kcal mol^{-1}) of the multifidene conformers from conformational map (torsional angles are in degrees).

Frames	ΔE	τ_1	τ_2	τ_3
I	0.0	170.0	120.0	−60.0
II	6.4	160.0	130.1	0.0
III	0.2	176.4	46.9	−30.0
IV	2.6	150.0	130.0	150.0
V	1.8	−129.9	120.0	180.0
VI	1.7	−99.9	130.0	180.0

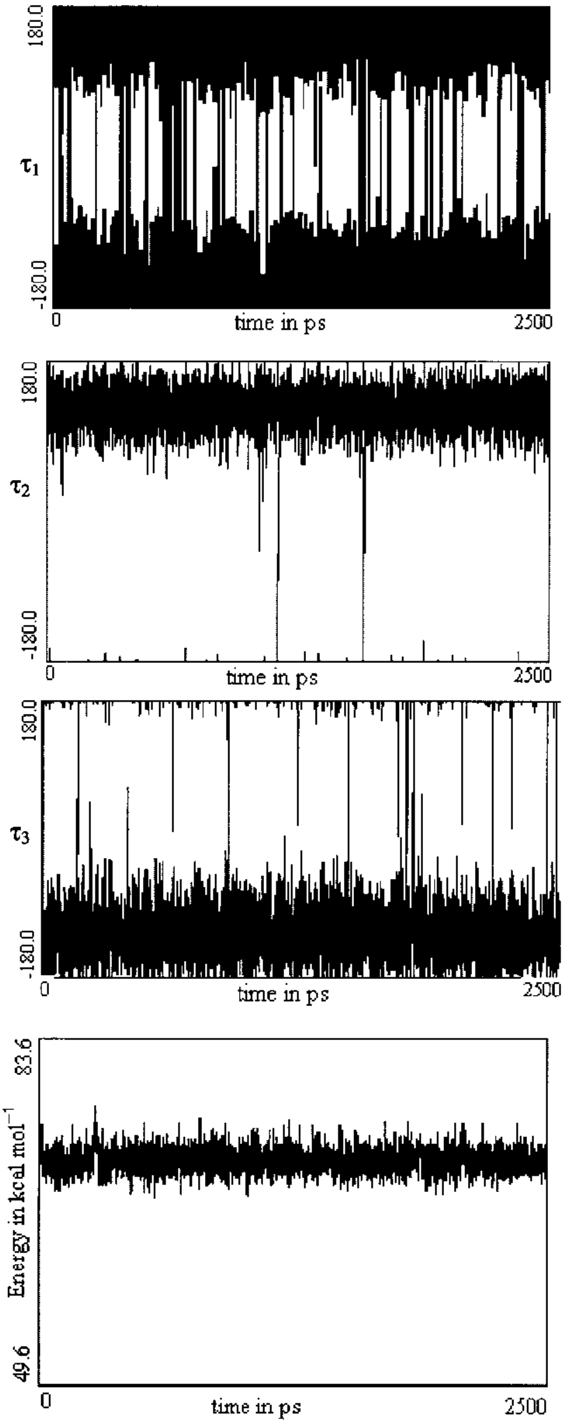

FIGURE 2 Evolution of τ_1, τ_2 and τ_3 torsional angles and energy as a function of time by molecular dynamics *in vacuo.*

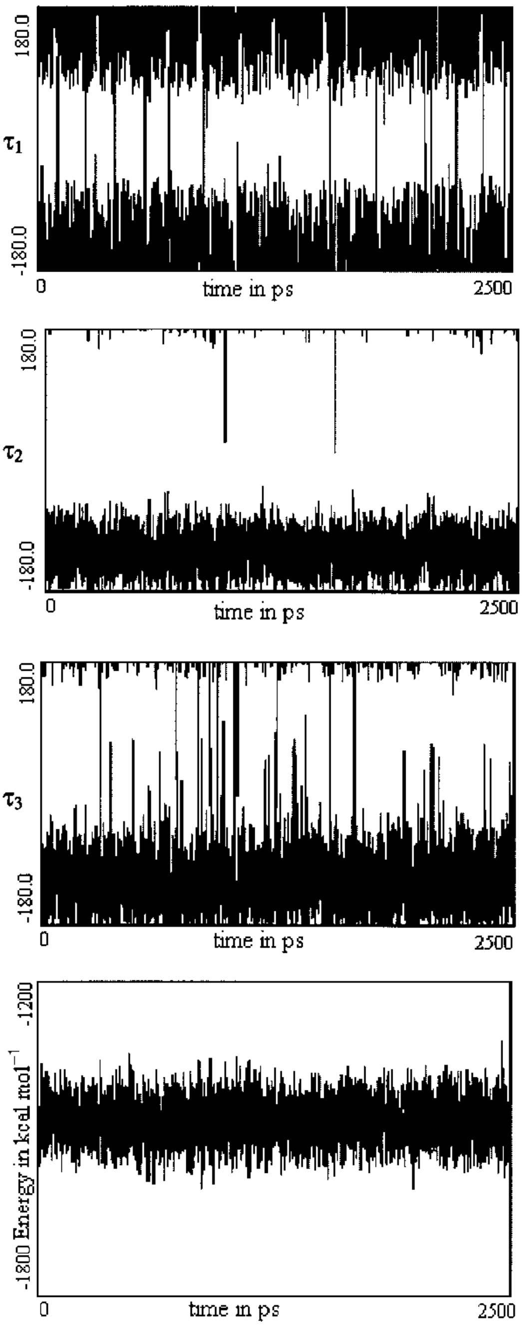

FIGURE 3 Evolution of τ_1, τ_2 and τ_3 torsional angles and energy as a function of time by molecular dynamics in water.

data. The computations were performed both *in vacuo* and in the presence of water using the polarizable continuum model fully optimizing the structures. To obtain information about the interconversion barriers between different minima, we also located the relative transition states. The results are listed in Tables III and IV. With both methods, all the starting

TABLE II Relative energies (ΔE in kcal mol^{-1}) of the multifidene conformers *in vacuo* and in water (torsional angles are in degrees).

Frames	ΔE	τ_1	τ_2	τ_3
MD in vacuo				
I	0.0	−99.5	−106.9	−140.8
II	0.1	−163.9	134.8	−140.8
III	1.9	102.3	−100.0	−130.9
IV	1.7	−98.0	−92.5	−140.8
V	2.1	−159.6	−109.9	−136.3
MD in water				
I	0.0	105.0	−121.7	−160.3
II	9.8	121.2	−100.5	95.3
III	16.4	114.3	−163.6	−139.3
IV	23.0	149.8	−145.5	−14.1
V	24.1	−158.4	−127.9	−147.7
VI	24.4	−141.9	−106.4	−88.2

conformations from MM and MD simulations gave only three minima (Fig. 4). The other conformations collapsed in one of these during the optimization steps. Both *in vacuo* and in solution, the absolute minimum was found to be the same with the two methods. The same results were obtained for the relative minima that follow the same energetic trend with respect to the absolute one. Going from *in vacuo* to solvent computations, it is worth noting that the ΔE increases approximately three-fold for the conformer B, while a less pronounced change was observed for the relative minimum C. Looking at the free solvation energy values, we note that the A and C minima were better solvated than the B minimum. Analysis of the different energetic terms in the ΔG expression revealed that this difference was essentially due to the electrostatic part being the non-electrostatic terms (cavitation, dispersion and repulsion) constant in all the three conformers. As shown in Tables III and IV, the geometries of the minima at B3LYP and MP2 levels were very similar, and the effect of the solvent, simulated by the polarizable continuum model method, was negligible in all three structures. The structure A can interconvert into structure B throughout a rotation around the dihedral angle τ_3, while B can be converted to C via a rotation around τ_2. We searched the transition states corresponding to these two paths, but only that corresponding to the A → B ($TS_{A\text{-}B}$) interconversion has been characterized. All the attempts to find the $TS_{B\text{-}C}$, corresponding to the B → C interconversion, failed. It may be that the explicit inclusion of some water molecules in the solvent description is necessary. The structure of $TS_{A\text{-}B}$, reported in Figure 4, shows that τ_1 and τ_3 assumed values of 2.3°

TABLE III Relative energies at 0 K (ΔE in kcal mol^{-1}) in gas phase (B3LYP/6-311++G**) and in solvent (B3LYP/6-311++G**/SCRF/PCM) for minima and maxima on the potential-energy surface of multifidene (torsional angles are in degrees).

	*B3LYP/6-311++G***				*B3LYP/6-311++G**/SCRF/PCM*			
	ΔE	τ_1	τ_2	τ_3	ΔE	τ_1	τ_2	τ_3
A	0.0	119.9	−122.9	−118.5	0.0	118.7	−121.3	115.1
B	2.3	119.8	−116.8	7.8	6.4	119.0	−115.1	8.0
C	6.7	−125.4	177.1	−2.1	7.9	−121.3	175.0	−2.6
$TS_{A\to B}$	2.7	2.3	−123.8	−65.9	–	–	–	–
$TS_{B\to C}$	–	–	–	–	–	–	–	–

TABLE IV Relative energies at 0 K (ΔE in kcal mol^{-1}) in gas phase (MP2/6-311++G**) and in solvent (MP2/6-311++G**/SCRF/PCM) for minima and maxima on the potential-energy surface of multifidene (torsional angles are in degrees).

	*MP2/6-311++G***				*MP2/6-311++G**SCRF/PCM*			
	ΔE	τ_1	τ_2	τ_3	ΔE	τ_1	τ_2	τ_3
A	0.0	116.7	−121.2	−120.2	0.0	115.1	−120.0	−118.0
B	1.9	116.8	−115.3	15.5	5.2	114.8	−113.4	14.5
C	5.1	−99.3	115.6	−1.2	7.2	−98.1	114.1	−0.9
$TS_{A\rightarrow B}$	2.6	0.6	−123.5	−70.4	–	–	–	–
$TS_{B\rightarrow C}$	–	–	–	–	–	–	–	–

and −65.9°, respectively, while the remaining dihedral angle τ_2 essentially retained the value of the A conformer at both levels of theory. The energy barrier for the A → B interconversion was only 2.7 (B3LYP) and 2.6 (MP2) kcal mol^{-1}, indicating that the interconversion could occur with a very low energy expense.

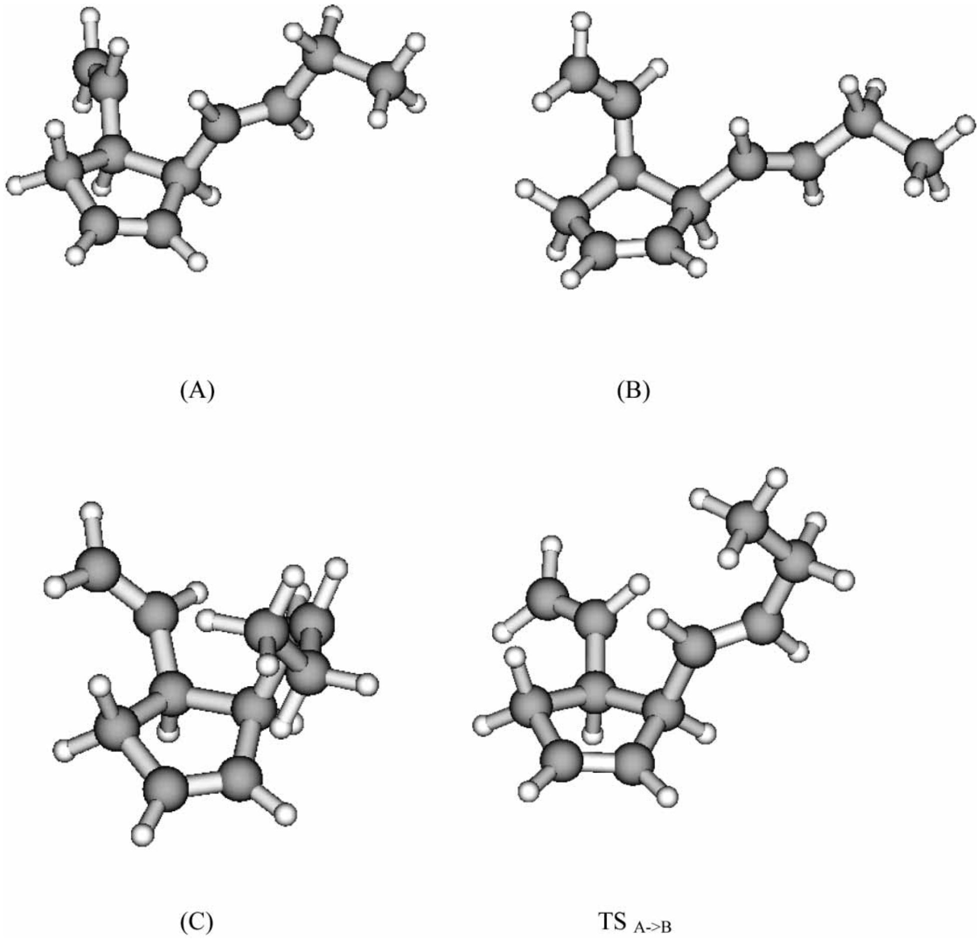
(A) (B) (C) TS A->B

FIGURE 4 Minima obtained at B3LYP and MP2 levels.

Since knowledge of the molecular charge distribution, together with the molecular shape and the conformational properties, plays a crucial role in the selectivity and function of biologically active systems, we also computed the atomic net charges in multifidene. We hope that this additional information can help the characterization of the receptor site and, consequently, yield better information on the molecular recognition process. Our results obtained from the natural bond order analysis (Reed *et al.*, 1988) performed at the B3LYP level show that the stronger negative electronic charge is located on the methyl group carbon (-0.56 |e|) of the longest aliphatic chain, followed by the carbon in the $-CH_2-$ group of the ring (-0.41 |e|) and the carbon of the methyl moiety in the other aliphatic chain (-0.38 |e|). These three negative centres are the most probable candidates for the interaction with the corresponding positive site on the receptor.

From Tables II–IV, it is evident that there is a good agreement between the MD, B3LYP and MP2 methods in predicting the absolute minimum, although some relative minima found in MD computations are not present in both the first-principle computations.

4 CONCLUSIONS

In this paper, we have performed a detailed conformational analysis of the multifidene molecule, employing different classical and quantum-mechanical tools such as molecular mechanics and dynamics, MP2 and density-functional methods. The main features of our investigations can be summarized as follows:

- The multifidene is a flexible molecule from a conformational point of view.
- Some minima found at the MM and MD level are not confirmed at a more rigorous MP2 and B3LYP level of theory.
- The located transition state corresponds to a very low potential energy barrier for the interconversion between the two minima.
- Solvent effects as described by PCM are negligible with respect to the structures of the minima; on the contrary, the explicit inclusion of water molecules in the MD simulation affects the relative energies between the conformers.

Acknowledgements

This work has been done in the framework of the MEMOBIOMAR-MIUR project.

References

Albano, M., Russo, N. and Toscano, M. (1991). Conformational analysis of multifidene and its synthetic analogues, in: Rizzarelli, E. and Theophanides, T. (eds.), *Chemistry and Properties of Biomolecular Systems*. Kluwer, Dordrecht, The Netherlands; pp. 23–33.

Barone, V. and Cossi, M. (1998). Quantum calculation of molecular energies and energy gradients in solution by a conductor solvent model. *The Journal of Physical Chemistry A*, **102**, 1995–2001.

Barone, V., Cossi, M. and Tomasi, J. (1998). Geometry optimization of molecular structures in solution by the polarizable continuum model. *Journal of Computational Chemistry*, **19**, 404–417.

Becke, A. D. (1993). Density-functional thermochemistry. III. The role of exact exchange. *The Journal of Chemical Physics*, **98** (7), 5648–5652.

Boland, W. (1995). The chemistry of gamete attraction: chemical structures, biosynthesis, and (a)biotic degradation of algal pheromones. *Proceedings of the National Academy of Sciences of the United States of America*, **92**, 37–43.

Boland, W., Jaenicke, L. and Mueller, D. G. (1981). Synthesis and biological activities of (+)- and (−)-multifidene. *Liebigs Annalen der Chemie*, **12**, 2266–2271.

Boland, W., Marner, F. J., Jaenicke, L., Mueller, D. G. and Foelster, E. (1983a). Comparative receptor study in gamete chemotaxis of the seaweeds *Ectocarpus siliculosus* and *Cutleria multifida*. *European Journal of Biochemistry*, **134**, 97–103.

Boland, W., Mertes, K., Jaenicke, L., Mueller, D. G. and Foelster, E. (1983b). 187. Absolute configuration of multifidene and viridiene, the sperm releasing and attracting pheromones of brown algae. *Helvetica Chimica Acta*, **66**, 1905–1914.

Boland, W., Pohnert, G. and Maier, I. (1995). Pericyclic reactions in nature: spontaneous cope rearrangement inactivates algae pheromones. *Angewandte Chemie International Edition English*, **34**, 1602–1604.

Bradley, S. M. (1999). Biosynthesis of marine natural products: microrganisms and macroalgae. *Natural Products Report*, **16**, 653–674.

Burks, J. E. and Crandall, J. K. (1984). Synthesis of cis vicinally disubstituted cyclopentanes by fragmentation of bicyclo[3.2.0]heptan-6-ols. Total synthesis of (+/−)-multifidene. *Journal of Organic Chemistry*, **49**, 4663–4670.

Crouse, G. D. and Paquette, L. A. (1981). Total synthesis of (+/−)-multifidene, the gamete attractant of the phaeophyte *Cutleria multifida. Journal of Organic Chemistry*, **46**, 4272–4274.

Dauber-Osguthorpe, P., Roberts, V. A., Osguthorpe, D. J., Wolff, J., Genest, M. and Hagler, A. T. (1988). Structure and energetics of ligand-binding to proteins: *Escherichia coli* dihydrofolate reductase/trimethoprim, a drug-receptor system. *Protein: Structure, Function, Genetic*, **4**, 31.

Ellis, J. M. and King, S. B. (2002). Ring-opening cross metathesis of 1,3-cyclopentadiene-heterodienophile cycloadducts to produce cyclic hydrazines and hydroxylamines. *Tetrahedron Letters,* **43**, 5833–5835.

Frisch, M. J., Trucks, G. W., Schlegel, H. B., Scuseria, G. E., Robb, M. A., Cheeseman, J. R., Zakrzewski, V. G., Montgomery, J. A., Stratmann, R. E., Burant, J. C., Dapprich, S., Millam, J. M., Daniels, A. D., Kudin, K. N., Strain, M. C., Farkas, O., Tomasi, J., Barone, V., Cossi, M., Cammi, R., Mennucci, B., Pomelli, C., Adamo, C., Clifford, S., Ochterski, J., Petersson, G. A., Ayala, P. Y., Cui, Q., Morokuma, K., Malick, D. K., Rabuck, A. D., Raghavachari, K., Foresman, J. B., Cioslowski, J., Ortiz, J. V., Stefanov, B. B., Liu, G., Liashenko, A., Piskorz, P., Komaromi, I., Gomperts, R., Martin, R. L., Fox, D. J., Keith, T., Al-Laham, M. A., Peng, C. Y., Nanayakkara, A., Gonzalez, C., Challacombe, M., Gill, P. M., Johnson, B. G., Chen, W., Wong, M. W., Andres, J. L., Head-Gordon, M., Replogle, E. S. and Pople, J. A. (1998). *Gaussian 98 (Revision A.1)*. Gaussian, Pittsburgh, PA.

Hemamalini, S. and Scheffold, R. (1995). Synthesis of (+)-multifidene. *Helvetica Chimica Acta,* **78**, 447–451.

Lebreton, J., Alphand, V. and Furstoss, R. (1996). A short chemoenzymatic synthesis of (+)-multifidene and (+)-viridiene. *Tetrahedron Letters*, **37**, 1011–1014.

Lee, C., Yang, W. and Parr, R. G. (1988). Development of the Colle-Salvetti correlation-energy formula into a functional of the electron density. *Physical Review B*, **37**, 785–789.

Marino, T., Russo, N., Tocci, E. and Toscano, M. (2001). Molecular dynamics, density functional and second order Moller-Plesset theory study of the structure and conformation of acetylcholine *in vacuo* and in solution. *Theoretical Chemistry Accounts*, **107**, 8–14.

Paquette, L. A., Coghlan, M. J. and Hayes, P. C. (1984). Absolute configuration of multifidene as deduced by total synthesis of the unnatural levorotatory enantiomer. *Journal of Organic Chemistry*, **49**, 4516–4518.

Randall, M. L. and Snapper, M. L. (1998). Selective olefin metatheses – new tools for the organic chemist: A review. *Journal of Molecular Catalysis A: Chemical*, **133**, 29–40.

Randall, M. L., Tallarico, J. A. and Snapper, M. L. (1995). Selective ring-opening cross-metathesis. Short syntheses of multifidene and viridiene. *Journal of the American Chemical Society,* **117**, 9610–9611.

Reed, A. E., Curtiss, L. A. and Weinhold, F. (1988). Intermolecular interactions from a natural bond orbital, donor-acceptor viewpoint. *Chemical Review*, **88**, 899–926.

Stanley, M. R. and Wan, P. W. H. (1998). Enzyme-catalysed Baeyer–Villiger oxidations. *Journal of Molecular Catalysis B: Enzymatic*, **4**, 111–136.

Tomasi, J. and Persico, M. (1994). Interactions in solution: an overview of methods based on continuous distribution of the solvent. *Chemical Review*, **94**, 2027–2094.

Villa, A., Fantucci, P., Marino, T. and Russo, N. (1995). Conformational behaviour of the antineoplastic peptide dolastatin-10 and of two mutated derivatives. *Journal of Computer-Aided Molecular Design*, **9**, 425–438.